Mon. Not. R. Astron. Soc. **346,** 319–326 (2003)

The power spectrum amplitude from clusters revisited: σ_8 using simulations with pre-heating and cooling

Pedro T. P. Viana,[1,2] Scott T. Kay,[3] Andrew R. Liddle,[3⋆] Orrarujee Muanwong[3,4] and Peter A. Thomas[3]

[1]*Centro de Astrofísica, Universidade do Porto, Rua das Estrelas, 4150-762 Porto, Portugal*
[2]*Departamento de Matemática Aplicada, Faculdade de Ciências, Universidade do Porto, Rua do Campo Alegre, 687, 4169-007 Porto, Portugal*
[3]*Astronomy Centre, University of Sussex, Falmer, Brighton BN1 9QJ*
[4]*Department of Physics, Faculty of Science, Khon Kaen University, Khon Kaen, 40002, Thailand*

Accepted 2003 August 5. Received 2003 July 18; in original form 2002 November 8

ABSTRACT

The amplitude of density perturbations, for the currently-favoured ΛCDM cosmology, is constrained using the observed properties of galaxy clusters. The catalogue used is that of Ikebe et al. The relation of cluster temperature to mass is obtained via *N*-body/hydrodynamical simulations including radiative cooling and pre-heating of cluster gas, which we have previously shown to reproduce well the observed temperature–mass relation in the innermost parts of clusters. We generate and compare mock catalogues via a Monte Carlo method, which allows us to constrain the relation between X-ray temperature and luminosity, including its scatter, simultaneously with cosmological parameters. We find a luminosity–temperature relation in good agreement with the results of Ikebe et al., while for the matter power spectrum normalization, we find $\sigma_8 = 0.78^{+0.30}_{-0.06}$ at 95 per cent confidence for $\Omega_0 = 0.35$. Scaling to the *Wilkinson Microwave Anisotropy Probe* central value of $\Omega_0 = 0.27$ would give a best-fitting value of $\sigma_8 \simeq 0.9$.

Key words: hydrodynamics – methods: *N*-body simulations – galaxies: clusters: general – X-rays: galaxies: clusters.

1 INTRODUCTION

It has recently become apparent that traditional hydrodynamical simulations, where the gas is only allowed to heat adiabatically and through shocks, have difficulties in matching observations in the central regions of clusters, with a significant underestimation of the temperature corresponding to a given cluster mass. This is potentially important for attempts to use the observed temperature function of clusters to constrain the matter power spectrum on short scales, a topic which has been studied by many authors over the years (Evrard 1989; Henry & Arnaud 1991; Oukbir & Blanchard 1992; White, Efstathiou & Frenk 1993a; Eke, Cole & Frenk 1996; Viana & Liddle 1996; Viana & Liddle 1999, hereafter VL99; Henry 1997, 2000; Blanchard et al. 2000; Pierpaoli, Scott & White 2001; Wu 2001), most of whom use hydrodynamical simulations to relate mass to temperature. Such concerns have been given further impetus by a recent paper by Seljak (2002), who used an observed relationship between cluster temperature and mass (Finoguenov, Reiprich & Böhringer 2001), rather than one derived from hydrodynamical simulations, to find a normalization for the matter power spectrum significantly lower than that of earlier works. In a recent paper (Thomas et al. 2002) we have shown that the inclusion of extra gas physics, namely radiative cooling of the gas and possible pre-heating of the gas before cluster formation, can bring simulations into good agreement with recent *Chandra* observations of the cores of clusters (Allen, Schmidt & Fabian 2001), suggesting that these may be crucial ingredients in obtaining an accurate description of clusters.

In this paper, we derive a constraint on the matter power spectrum normalization σ_8 in a way which improves on previous work in several ways. On the theoretical side, we incorporate the temperature–mass relationship, and its scatter, as obtained from the simulations described above. On the observational side, we compare with the data published in Ikebe et al. (2002), whose raw catalogue contains around 100 clusters, most with data from both *ROSAT* and *ASCA*. Finally, on the data analysis side we use a novel approach, whereby Monte Carlo simulations are used to generate mock galaxy cluster catalogues, which through comparison with the data published in Ikebe et al. (2002) lead to a simultaneous constraint on the relationship of X-ray temperature to luminosity, including its scatter, and on the matter power spectrum normalization σ_8.

⋆E-mail: a.liddle@sussex.ac.uk

2 THE OBSERVED CLUSTER CATALOGUE

The galaxy cluster catalogue containing the best available X-ray data is that compiled by Ikebe et al. (2002) and Reiprich & Böhringer (2002). The master catalogue contains 106 clusters, selected by their X-ray *ROSAT* flux from available cluster catalogues, with 88 among them having been observed by *ASCA*. Imposing a flux cut in the *ROSAT* [0.1, 2.4] keV band of 2.0×10^{-11} erg s^{-1} cm^{-2}, a flux-limited sample of 63 clusters is then obtained, called HIFLUGCS, which is claimed to be statistically complete (Reiprich & Böhringer 2002). Ikebe et al. (2002) use a slightly different sample in their analysis, obtained by excluding the two lowest temperature clusters from HIFLUGCS, ending up with a sample of 61 clusters with X-ray temperatures ranging from 1.4 up to 11 keV. Among these, 56 have X-ray temperatures derived by Ikebe et al. (2002) from *ASCA* data by means of a two-temperature model that takes into account a possible contribution from a cooler component at the cluster core.

In order to define the observed cluster sample with which to compare the artificially-generated cluster catalogues, we will impose more restrictive selection criteria on HIFLUGCS than Ikebe et al. (2002) did. We will only consider clusters with measured X-ray flux in the [0.1, 2.4] keV band above 2.2×10^{-11} erg s^{-1} cm^{-2}, X-ray temperature higher than 2 keV, and a redshift between 0.03 and 0.10 (when performing tests, we found that including clusters with $z < 0.03$ seems to lead to an increase in the best-fitting σ_8 by a few per cent). These ranges were chosen to maximize confidence in completeness of the sample, to minimize cosmic variance, and because the luminosity–temperature relation is expected to deviate from a power law below 2 keV due to non-gravitational physics.

So that we can account for the measurement errors both in flux and temperature, which can lead to incompleteness effects when imposing either flux or temperature criteria in the sample selection procedure, we used Monte Carlo simulations to generate 40 realizations of the HIFLUGCS catalogue, with the measurement errors in flux and temperature modelled as Gaussian distributed. We then imposed our cluster selection criteria, described above, on these catalogues to obtain a set of 40 observed cluster samples, with very similar but not identical numbers of clusters, representing different possible realizations of the chosen observed cluster sample.

We performed extensive tests to determine the minimum number of Monte Carlo realizations of HIFLUGCS that should be generated, so as to properly account for the effect of the measurement errors on the distribution of the cluster properties, within the observed data sample which we will use to compare with the artificially-generated cluster catalogues. We found that 40 realizations are enough, and increasing their number to 200 or 1000 has a negligible effect both on the typical distribution of cluster properties and on the final probability distribution for σ_8. We also generated bootstrap realizations of HIFLUGCS, to determine whether the flux and temperature measurement errors provided by Ikebe et al. (2002) were realistic. They seem to be, given that the bootstrap realizations share the same mean statistical properties as the Monte Carlo ones, leading to negligible differences in the final probability distribution of σ_8 values. Finally, there does not seem to be any systematic shift in the mean statistical properties of both the Monte Carlo and bootstrap catalogues with relation to HIFLUGCS, which is reflected by the fact that our result on σ_8 does not change even if we just apply our selection criteria to HIFLUGCS, and then compare the resulting cluster sample with the artificially-generated cluster catalogues.

3 THE MOCK CLUSTER CATALOGUES

The direct simulation of X-ray cluster catalogues from hydrodynamical simulations is beyond present computational means due to the excessive number of particles required to obtain statistically-robust cluster abundances with temperatures above a few keV. Instead, we appeal to the method used by Holder, Haiman & Mohr (2001), which is to use generalized mass functions of dark matter haloes to generate catalogues of clusters identified by their redshift and mass, and then estimate their X-ray temperatures using the mass–temperature relation of clusters in hydrodynamical simulations. With relation to previous work, the main improvement in this paper is the use of a mass–temperature relation that is drawn from simulations with more detailed models of the intracluster gas physics than have previously been implemented, and which closely match the X-ray properties of observed clusters (Thomas et al. 2002; Muanwong et al. 2002, hereafter MTKP02).

3.1 The mass function

Currently no standard definition of a dark matter halo exists, although it is convenient to define a halo as an overdense concentration of matter using the results of the spherical top-hat collapse model (STHCM; e.g. Peebles 1993; although see also Sheth, Mo & Tormen 2001). For $\Omega = 1$, the boundary of a halo predicted by the STHCM contains a mean internal overdensity of $18\pi^2 \approx 178$ relative to the critical density. This result has led many authors to define haloes using an overdensity contrast of 200 (which we take as our fiducial case). Note that even with the current generation of X-ray satellites it is not feasible to measure spatially-resolved properties of clusters to such large radii.

A comprehensive study of the mass function of cold dark matter (CDM) haloes was carried out by Jenkins et al. (2001, hereafter Jen01), who compared results from the largest N-body simulations available (the Hubble Volume simulations simulated by the Virgo Consortium, which used sufficiently large volumes to obtain reliable abundances of haloes on scales corresponding to rich clusters of galaxies) to the mass function predicted by Press & Schechter (1974). They demonstrated that the simulated mass function predicts a lower abundance of haloes at low masses than the Press–Schechter function, but a higher abundance at high masses. Although they did not investigate the cause of this discrepancy, they pointed out that the Press–Schechter Ansatz that all mass is contained in bound objects is untrue in the simulations for conventional halo definitions.

Jen01 produced fits to simulated mass functions using two different estimators: the spherical-overdensity (SO) and friends-of-friends (FOF) algorithms. The first case, as implemented by Lacey & Cole (1994), finds and ranks the densest dark matter particles and, starting from the densest, grows a sphere until the mean internal density equals some multiple of the critical density, $\rho_{\rm cr}$, $\langle\rho\rangle = \Delta\rho_{\rm cr}$. Particles within this halo are then removed from the list and the procedure is repeated until all haloes are found down to a given mass limit. The FOF algorithm (Davis et al. 1985) links particles together using a fixed linking length of $bn^{-1/3}$, where n is the mean particle density. The FOF algorithm does not impose spherical symmetry on the shapes of the haloes (which are typically triaxial) but can sometimes link together haloes which are in close proximity. It is important to use a consistent definition for cluster masses to define both the mass function and the mass–temperature relation; failure to do so can lead to errors of 10 per cent in the derived value of σ_8.

A further result from the Jen01 analysis was that the mass functions, when expressed as a function of $\ln(\sigma^{-1})$ (where $\sigma(M)$ is the generalization of σ_8 to any mass scale), are independent of cosmology if haloes are defined using either a fixed linking length (e.g. $b = 0.2$) in the FOF case or defining the SO threshold with respect to the mean background density (e.g. $\Delta = 180\Omega_0$) in the SO case. This was confirmed by Evrard et al. (2002, hereafter Evr02), who also provided fits (as a function of Ω) to simulated mass functions using a SO algorithm with $\Delta = 200$ (i.e. overdensity measured with respect to the critical density). For this paper, we adopt M_{200} as the fiducial definition of cluster mass, and use the Evr02 fits to estimate the mass function at different $\Omega(z)$. We have checked that our method for measuring cluster masses from the simulations (required for the calibration of the mass–temperature relation) produces almost identical results to the SO method used by Jen01 and Evr02 (the median difference in halo masses is less than 0.5 per cent).

3.2 The mass–temperature relation

In this section, we use results drawn from simulations carried out using the HYDRA[1] N-body/hydrodynamics code (Couchman, Thomas & Pearce 1995; Pearce & Couchman 1997) on the Cray T3E computer at the Edinburgh Parallel Computing Centre as part of the Virgo Consortium[2] programme of investigations into structure formation in the Universe. Details of the method and choice of simulation parameters were discussed by MTKP02; we summarize details pertinent to the results of this paper below.

We adopt the currently-favoured ΛCDM cosmological model, setting the density parameter $\Omega_0 = 0.35$, cosmological constant $\Omega_\Lambda = 0.65$, baryon density $\Omega_b = 0.038$, Hubble parameter $h = 0.71$ and linear power spectrum shape parameter $\Gamma = 0.21$. The purpose of this paper is to provide constraints on σ_8 and so it may seem premature to pick one particular value for our simulations. However, the mass–temperature relation of clusters is largely independent of σ_8. The simulations presented in MTKP02 use $\sigma_8 = 0.9$; we have subsequently repeated one of the simulations with a lower normalization, $\sigma_8 = 0.7$, and find an identical relation within the uncertainties.

MTKP02 presented three simulations which differed in the way in which the gas was heated and cooled. In the first simulation, a *non-radiative* model, the gas could undergo heating by adiabatic compression and shocks but could not cool radiatively. Consequently, the resulting clusters are far too luminous for their mass and so do not agree with observed X-ray scaling relations (MTKP02). We do not use results from this simulation.

In the *radiative* simulation, gas was able to cool radiatively using the collisional ionization equilibrium tables of Sutherland & Dopita (1993). Cooled material was permitted to form stars, removing low-entropy material with short cooling times from the centres of the clusters. Finally, in the *pre-heating* simulation (which also includes cooling), the specific thermal energy of the gas was raised by 1.5 keV per particle at $z = 4$, to crudely model the effects of energy injection by galactic winds. Both models reproduce key X-ray cluster scaling relations at $z = 0$, although the former predicts too much cooled gas (i.e. stars and galaxies) compared to observations and the latter too little.

We estimate the X-ray temperature of each cluster by weighting the contribution from each hot gas ($T > 10^5$ K) particle by its bolometric flux

$$T_X = \frac{\Sigma_i m_i \rho_i \Lambda_{\rm bol}(Z, T_i) T_i}{\Sigma_i m_i \rho_i \Lambda_{\rm bol}(Z, T_i)}. \quad (1)$$

Here, m_i, ρ_i and T_i are the mass, density and temperature of the particles, respectively, $Z = 0.3\ {\rm Z}_\odot$ is their metallicity and $\Lambda_{\rm bol}$ is the bolometric cooling function from Sutherland & Dopita (1993). Adopting a soft-band cooling function (appropriate for *ROSAT* observations) makes no significant difference to the estimated temperature. Many clusters show enhanced emission from the cluster core that has a lower temperature than the cluster mean (MTKP02). For this reason, we present results for the mass–temperature relation both including and excluding the X-ray emission from within the 'cooling radius', defined as the radius within which the mean cooling time of the gas is 6 Gyr. The latter results are referred to as 'cooling-flow corrected'.

Table 1. Power-law fits to the simulated mass–temperature relations of X-ray clusters: cluster sample; number of clusters in sample; slope of relation, s; rms dispersion in temperature about best fit (see text); value of $M_{200}/10^{14}\ h^{-1}\ {\rm M}_\odot$ at 3 keV; value of $M_{200}/10^{14}\ h^{-1}\ {\rm M}_\odot$ at 6 keV.

Sample	N	s	rms	M_{200}@3	M_{200}@6
All data					
Radiative	36	1.80	0.092	2.9	10.1
Pre-heating, $\sigma_8 = 0.9$	31	1.59	0.056	2.4	7.3
Pre-heating, $\sigma_8 = 0.7$	12	1.75	0.049	2.1	7.1
Pre-heating, $\sigma_8 =$ any	43	1.61	0.053	2.4	7.3
Cooling-flow corrected					
Radiative	36	1.55	0.079	2.3	6.8
Pre-heating, $\sigma_8 = 0.9$	31	1.51	0.054	2.2	6.2
Pre-heating, $\sigma_8 = 0.7$	12	1.70	0.040	2.4	7.7
Pre-heating, $\sigma_8 =$ any	43	1.54	0.049	2.2	6.4

In Table 1, we list parameters for the straight-line relation of the form

$$\log(kT/{\rm keV}) = {\rm const} + (1/s) \log\left(M_{200}/h^{-1}\,{\rm M}_\odot\right) \quad (2)$$

that minimizes the dispersion in temperature for all clusters with $\log(M_{200}/h^{-1}\,{\rm M}_\odot) > 14$. The column labelled 'rms' gives the root-mean-square dispersion in the log of temperature (for $N - 2$ degrees of freedom) about the best-fitting line. We have also measured this dispersion for clusters in a lower mass range, $13.7 < \log(M_{200}/h^{-1}\,{\rm M}_\odot) < 14$, and find very similar values. Hence we will assume in our analysis that the dispersion is independent of mass.

The final two columns of Table 1, labelled M_{200}@3 and M_{200}@6, give the values of the mass, in units of $10^{14}\ h^{-1}\ {\rm M}_\odot$, for the best-fitting relation at temperatures of 3 and 6 keV. The numbers in the M_{200}@3 column are mostly very similar to each other, except for the top entry for clusters in the radiative simulation without the cooling-flow correction. The presence of cool gas in the cores of these clusters lowers the emission-weighted temperature and hence raises M_{200}@3. The slope of the mass–temperature relation for $\sigma_8 = 0.7$ is higher than that for $\sigma_8 = 0.9$ but the two are in agreement to within the errors; with only 12 clusters covering a limited mass range, the formal 1-sigma error in the slope for the $\sigma_8 = 0.7$ clusters is about ± 0.4. The predictions for the normalizations of the relations at 6 keV are less certain, especially for $\sigma_8 = 0.7$, because they require a degree of extrapolation beyond the temperature range of the simulated data. For this reason, the difference between the cooling-flow corrected normalizations at 6 keV for $\sigma_8 = 0.7$ and $\sigma_8 = 0.9$ should not be taken too seriously. We use the combined catalogue for our analysis in the next section, but note that very

[1] See http://hydra.susx.ac.uk/
[2] See http://virgo.susx.ac.uk/

Table 2. Mass–temperature relations of X-ray clusters from previous simulations: paper (Evrard et al. 1996, EMN96; Bryan & Norman 1998, BN98; Thomas et al. 2001, T01; Mathiesen & Evrard 2001, ME01; slope of relation, s; value of $M_{200}/10^{14}\,h^{-1}\,\mathrm{M}_\odot$ at 3 keV; value of $M_{200}/10^{14}\,h^{-1}\,\mathrm{M}_\odot$ at 6 keV.

Paper		s	M_{200}@3	M_{200}@6
EMN96	Soft band	1.50	2.3	6.5
BN98	Bolometric	1.50	3.6	10.2
T01	Bolometric	1.50	2.5	7.1
ME01	Bolometric	1.39	4.0	10.6

similar results are obtained if we use the $\sigma_8 = 0.9$ relation instead.

In Table 2 we present results from several earlier studies of the mass–temperature relation in non-radiative simulations. Note that these results have been obtained by rescaling, when needed, the cluster mass to M_{200} (using a NFW profile; Navarro, Frenk & White 1995, 1996, 1997) and to the cosmology being considered here (as in Bryan & Norman 1998, hereafter BN98). Clearly there is a wide range of normalizations. This mainly results from the different resolutions of the simulations – although in the case of Evrard, Metzler & Navarro (1996, hereafter EMN96) their method of temperature estimation also plays a part. Also, on average, at fixed temperature the cluster masses in Table 2 are higher than those in Table 1. This is due to the absence of radiative cooling; cluster cores are full of dense, cold gas with short cooling times and this leads to low emission-weighted temperatures. This problem is largely overcome in the radiative and pre-heating simulations and can be reduced even further by the omission of the cooling-flow component. For comparison, Viana & Liddle (1996, 1999) used a normalization for the present-day mass–temperature relation which corresponds to $M_{200} = 10.1 \times 10^{14}\,h^{-1}\,\mathrm{M}_\odot (kT/6\,\mathrm{keV})^{1.5}$, based on a simulation of a single high-mass cluster from White et al. (1993b). This agrees well with the results of BN98 and Mathiesen & Evrard (2001, hereafter ME01), but lies well above the values found by EMN96 and in the radiative and pre-heating simulations reported in this paper. This change in normalization forces the estimate of σ_8 downwards.

3.3 Mock catalogue construction

We are now in a position to be able to combine the Evr02 fits to the mass function with the information on the cluster mass–temperature relation from the hydrodynamical simulations, to produce mock cluster catalogues with information on cluster redshift, mass and X-ray temperature.

We take the present-day shape of the matter power spectrum to be well approximated by that of a CDM model, with scale-invariant primordial density perturbations and effective shape parameter, $\Gamma = 0.18$. This is the favoured value of Γ from a joint analysis of the 2dF (Percival et al. 2001) and the Sloan Digital Sky Survey (SDSS; Szalay et al. 2003; Dodelson et al. 2002) data, when accounting for both statistical and systematic uncertainties. (The allowed interval for Γ is [0.08, 0.28] and we confirmed that varying Γ within this interval does not significantly change the final results; changing Γ to either 0.08 or 0.28 leads to a variation of only 0.02 in the best-fitting σ_8, with a higher Γ implying a higher σ_8.)

We begin by estimating the mean number of clusters as a function of mass (M_{200}) and redshift, using the Evr02 fits to the mass function, for each value of σ_8 over the interval of interest. Our redshift bins cover the range [0.03, 0.10] in intervals of 0.001, and our mass bins cover the range $[0.1, 2.0] \times 10^{15}\,h^{-1}\,\mathrm{M}_\odot$ in logarithmically-spaced intervals of 0.01. (We have checked that our results are insensitive to smaller bin sizes.) The initial mock cluster catalogues are then produced by attributing to each (z, M_{200}) bin, a number of clusters drawn from a Poisson distribution whose mean is that predicted by the Evr02 fits to the mass function. We assign a mass and redshift to each individual cluster by randomly drawing the two quantities from a quadratic distribution that best reproduces the variation in the cluster numbers in the neighbourhood of that bin. In this manner, we produce 1000 mock catalogues for each interesting value of σ_8. Through extensive tests we have found that such number is enough to properly account for the effect of the Poisson noise, as increasing the number of mock catalogues per σ_8 to, for example, 10 000 had a negligible effect on the final probability distribution for σ_8.

Each cluster in the catalogues is given an X-ray temperature, randomly drawn from a Gaussian distribution in ($\log_{10} M_{200}$, $\log_{10} kT$), with mean obtained by substituting the cluster mass (multiplied by $H(z)/H_0 \propto \sqrt{\Omega_0(1+z)^3 + (1-\Omega_0)}$ to account for the redshift evolution in the normalization of the cluster X-ray temperature to mass relation; see ME01) in expression (2), while the dispersion is assumed to be independent of mass. We fix the present-day normalization, slope and dispersion of the mass–temperature relation using the joint cluster catalogue obtained from the pre-heating simulations, where the X-ray temperatures were cooling-flow corrected. (Using the parameters deduced from the radiative simulations does not change the final results significantly.) Our method approximately reproduces that used by Ikebe et al. (2002) to estimate the observed cluster temperatures. We then exclude from the 1000 mock catalogues any cluster whose X-ray temperature does not exceed 2 keV.

To compare our simulated catalogues with the data we still need to impose the chosen flux selection criterion, which forces us to use a relation between X-ray luminosity (in the [0.1, 2.4] keV rest-frame band) and temperature. In order to be consistent, we determine this relation from the data simultaneously with σ_8 (see also Diego et al. 2001). We take it to be a power law of the form

$$\log_{10}\left(L_\mathrm{X}/h^{-2}\,\mathrm{erg\,s^{-1}}\right) = A + \alpha \log_{10}(kT/\mathrm{keV}), \tag{3}$$

with a dispersion $\sigma_{\log_{10} L_\mathrm{X}}$ taken to be independent of temperature, and we construct a grid of values (with dimensions $21 \times 31 \times 16$) of the normalization A, slope α and dispersion. For each point in this grid, and for every one of the 1000 catalogues available for each σ_8, we create 50 realizations of the luminosity[3] for every cluster by randomly drawing from a Gaussian distribution in ($\log_{10} kT$, $\log_{10} L_\mathrm{X}$) with the appropriate mean and dispersion. Every cluster then has its X-ray flux in the rest-frame [0.1, 2.4] keV band derived, from which the flux in the observed [0.1, 2.4] keV band is estimated using K-correction formulae. The flux limit of 2.2×10^{-11} erg s^{-1} cm^{-2} is then imposed. This generates a set of 50 000 mock catalogues for each combination of the four parameters we wish to estimate from the data. In all, over twenty-five billion mock catalogues were generated.

4 RESULTS

We are now in possession of an ensemble of catalogues representing the observed data set, and a collection of mock catalogues for different values of both σ_8 and the parameters that characterize the

[3] Extensive tests have shown that such a number is enough to lead to a dense coverage of the range of possible luminosity distributions, and increasing the number of realizations to, for example, 200 had a negligible effect on the final probability distribution for σ_8.

X-ray luminosity–temperature relation. We chose to perform the comparison between the observed and theoretical catalogues via a (three-way) two-dimensional (2D) Kolmogorov–Smirnov (KS) test. This test is a generalization to 2D distributions of the traditional KS test, and is due to Fasano & Franceschini (1987), following an earlier idea of Peacock (1983). A very good description of the 2D KS test can be found in Press et al. (1992). In order to calculate the probability of each set of four free parameters being the correct one, we compare each of the observed catalogues with each mock catalogue, and then add the probabilities of each pair of catalogues being drawn from the same underlying distribution of cluster properties. The probability is taken to be zero if the two catalogues being compared do not have the same number of clusters, otherwise it is given by the product of the probabilities that result from applying the 2D KS test to the three available distributions of cluster properties: (z, kT), (z, $L_{\rm X}$) and (kT, $L_{\rm X}$). The set of free parameters considered most correct will thus be the one that most often closely reproduces the observed distribution of the cluster properties (z, kT, $L_{\rm X}$).

4.1 Methodology tests

As far as we are aware, the 2D KS test has not previously been applied in the same context as here. We chose to employ the KS test rather than the widely-used likelihood method because it allows a fairly simple incorporation of the selection effects entering the observations, and can allow for scatter in the cluster relations. Ikebe et al. (2002) employed the likelihood function, but did not include scatter in the mass–temperature relation, although Pierpaoli et al. (2003) were able to include the scatter in a likelihood analysis. We favour the 2D KS test because of its ease of implementation, although we do not expect it to lead to significantly different results from the likelihood method.

It is clearly important to compare the 2D KS test to the likelihood method. We do this by applying the two methods to a simplified situation using 1000 mock observational cluster catalogues (we checked that generating more does not affect the results of the comparison) produced using the Evr02 fits to the mass function in the same manner as described in Section 3.3, with each cluster being characterized by its redshift, z, and mass, M_{200}. The assumed fiducial model had $\Omega_0 = 0.35$, $\sigma_8 = 0.8$ and $\Gamma = 0.18$. The sky coverage was the same as that of HIFLUGCS and the redshift interval considered was $0.03 < z < 0.10$. The mock observational catalogues were produced assuming that all clusters with M_{200} above $4.6 \times 10^{14}\ h^{-1}\ {\rm M}_{\odot}$ are detected, and none below. In all they have on average 41 clusters (a number similar to the HIFLUGCS subsample we are working with).

When applying the 2D KS test to each of the 1000 mock observational catalogues, 1000 synthetic catalogues were produced for each σ_8 in the interval of interest [0.60, 1.00], thus overall around 4×10^7 catalogue comparisons were made. In this case, the likelihood function is the product of the Poisson probabilities of finding exactly one cluster in the element ${\rm d}M_{200}\,{\rm d}z$ at each of the (M^i_{200}, z^i) combinations present in the mock catalogues, and of finding zero clusters elsewhere in the (M_{200}, z) plane (see, for example, Marshall et al. 1983).

In Fig. 1 we show the probability distributions for σ_8 obtained by the two methods. This comparison shows that both methods are unbiased, picking up the fiducial $\sigma_8 = 0.8$ as the most probable value. Further, the shape of the two probability distributions is very similar, although applying the 2D KS test seems to result in slightly more conservative confidence limits. We have made simulations with other initial assumptions and the results do not change qualitatively.

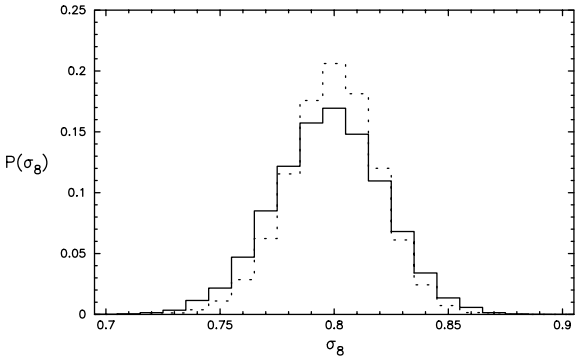

Figure 1. Marginalized probability distributions for σ_8, obtained through the 2D KS test (full line) and the likelihood method (dotted line).

4.2 Application to HIFLUGCS

The application of the 2D KS test to the HIFLUGCS data in the manner previously described results in the marginalized probability distributions, for each free parameter over the three others, presented in Figs 2 and 3. The histograms originate from the discretization of our parameter space (σ_8, A, α, $\sigma_{\log_{10} L_{\rm X}}$) for the Monte Carlo simulations. The continuous lines represent the most probable underlying probability density functions, and result from the application of a non-parametric smoothing technique to the histogram data. Note that these functions have been renormalized for easier comparison with the histograms. In summary

$$\sigma_8 \simeq 0.78 \quad \text{within} \quad [0.72, 1.08], \tag{4}$$

and

$$\log_{10}\left(L_{\rm X}/h^{-2}{\rm erg\,s^{-1}}\right) = A + \alpha \log_{10}(kT/{\rm keV}), \tag{5}$$

with

$$A \simeq 42.1, \quad \text{within} \quad [41.2, 42.5], \tag{6}$$

$$\alpha \simeq 2.5 \quad \text{within} \quad [1.5, 3.5], \tag{7}$$

$$\sigma_{\log_{10} L_{\rm X}} \simeq 0.3 \quad \text{within} \quad [0.0, 0.6]. \tag{8}$$

where the given ranges are all at the 95 per cent confidence level. The most probable combination of the four parameters we consider is $\sigma_8 = 0.77$, $A = 42.2$, $\alpha = 2.6$ and $\sigma_{\log_{10} L_{\rm X}} = 0.175$. Note that the distribution for σ_8 is considerably non-Gaussian, with the median value $\sigma_8 = 0.81$ being higher than the modal one. The tail

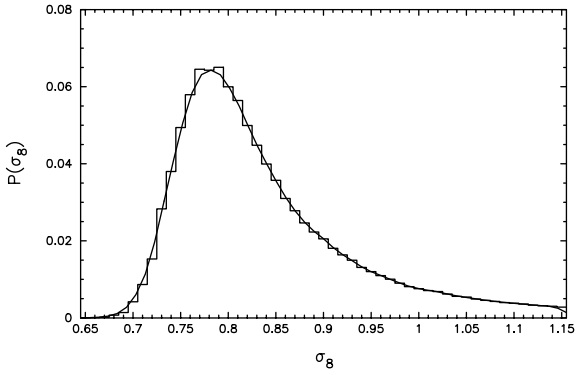

Figure 2. Marginalized probability distribution for σ_8, showing the bins as calculated and a smoothed version of the distribution.

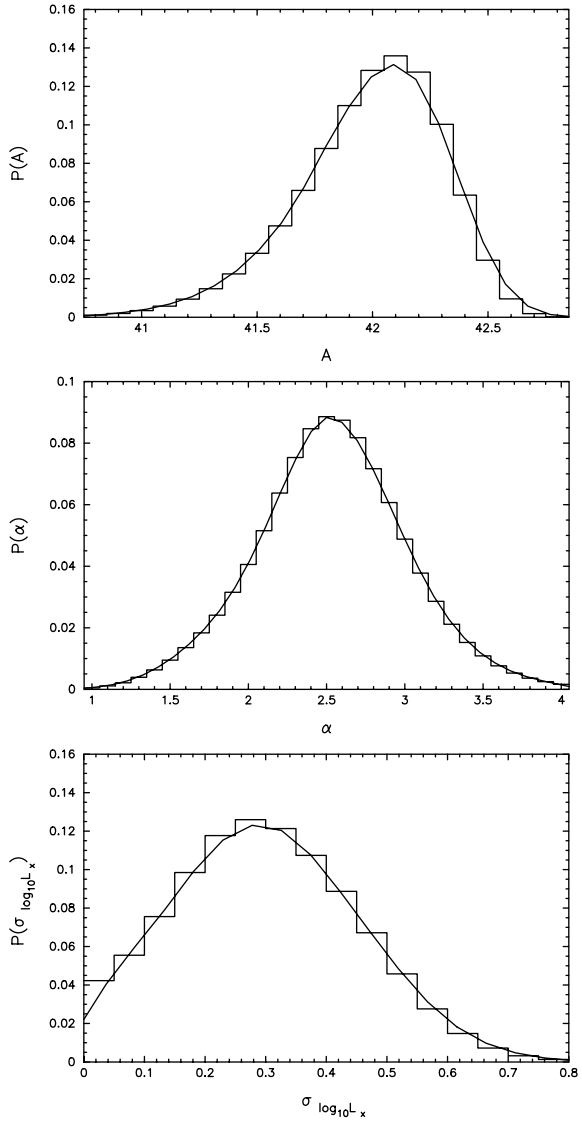

Figure 3. Marginalized probability distributions for the normalization A (top) and slope α (middle) of the relation between X-ray temperature and luminosity, as well as for its dispersion $\sigma_{\log_{10}L_X}$ (bottom).

extends much further to high σ_8 because, as the number of existing clusters increases, it remains possible to reproduce the observed number of clusters by simultaneously choosing lower values for A and higher values for $\sigma_{\log_{10}L_X}$. In the limit where no dispersion in the relation between X-ray luminosity and temperature is allowed, the possibility of σ_8 taking high values disappears, and the marginalized probability distribution for σ_8 becomes close to Gaussian. Re-doing our analysis not allowing for any dispersion in the relation between X-ray luminosity and temperature, the most probable value for σ_8 changes to 0.76, with the 95 per cent confidence interval now extending from 0.70 to 0.81, while the most probable values for the parameters A and α remain almost the same, changing to 42.3 and 2.6, respectively.

These results are similar to those obtained by Ikebe et al. (2002). The comparison between the two analyses is made difficult by the fact that they only indicate the most probable values for A, α and $\sigma_{\log_{10}L_X}$ for their best-fitting Ω_0 and σ_8, which are 0.26 and 0.94 respectively if only $T > 3$ keV clusters are considered. Concentrating on this case, and assuming $\Omega_0 = 0.26$ (plus $\Gamma = 0.206$, as in Ikebe et al. 2002), we attempted to recover the values obtained by Ikebe et al. (2002) for the other four parameters. We took into account that their assumed normalization for the cluster mass (M_{200}) to X-ray temperature relation (estimated as if $z = 0.05$) is higher, such that for a 3-keV cluster they assume a cluster mass around 4 per cent higher than us, while at 6 keV the difference increases to 13 per cent, as well as the fact that they do not take into account a possible dispersion in the cluster X-ray temperature at fixed mass. A most probable value of $\sigma_8 = 0.98$ was obtained by applying our procedure, with good agreement also found for the parameters A, α and $\sigma_{\log_{10}L_X}$. Given that some differences remain between the two analyses, our results thus seem to be consistent with those of Ikebe et al. (2002).

In order to determine which type of information in the data is driving the results, we determined the most probable values for the four parameters under consideration by applying in isolation the 2D KS test to the three available distributions of cluster properties: (z, kT), (z, L_X) and (kT, L_X). σ_8 is essentially unconstrained by the (z, L_X) distribution. All the information comes from the two others, with the (kT, L_X) distribution being slightly more constraining than the (z, kT) one. Consistently, the former prefers 0.78 as the most probable value for σ_8, while the latter settles for 0.79. The information on the parameters A, α and $\sigma_{\log_{10}L_X}$ is roughly equally distributed amongst the three distributions, although again (kT, L_X) and (z, L_X) are always the most and least constraining respectively, and when taken in isolation all three distributions lead to very similar results.

In Fig. 4 we compare the cluster properties between a realization of the HIFLUGCS subsample selected for the analysis, the mock sample that most resembles it, generated for the most probable set of parameters, and the underlying cluster population. Notice that the

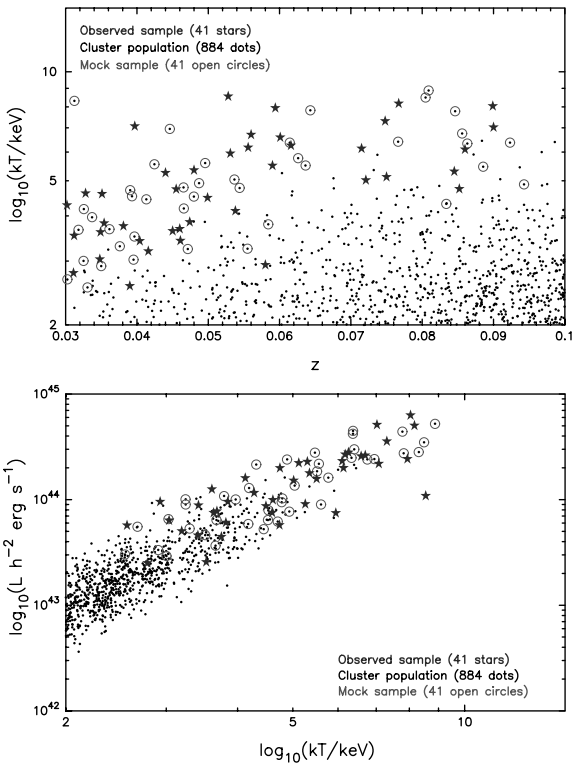

Figure 4. Comparison of distribution of cluster properties (T versus z, top; L_X versus T, bottom) between a realization of the HIFLUGCS subsample considered, the mock sample that most resembles it, generated for the most probable set of parameters, and the underlying cluster population.

incompleteness of the flux-limited samples increases considerably as the cluster X-ray temperature becomes lower, so that below an X-ray temperature of about 5 keV we can conclude that HIFLUGCS is vastly incomplete.

Our analysis is for $\Omega_0 = 0.35$, which is the value for which the large hydrodynamical simulations were run. The spectacular recent results from the *Wilkinson Microwave Anisotropy Probe* (*WMAP*; Bennett et al. 2003; Spergel et al. 2003) are consistent with this, but their best fit is lower at $\Omega_0 = 0.27$. While we are unable to run new large simulations, we can predict the effect on σ_8 using the scaling found in earlier analyses. VL99 found that for flat cosmologies $\sigma_8 \propto \Omega_0^{-0.47}$, and using this scaling we obtain a best-fitting σ_8 of 0.88 for $\Omega_0 = 0.27$. Given the small range over which this scaling is needed, the fractional uncertainty in σ_8 should be unchanged.

5 DISCUSSION

To set the context for the following discussion, we first remind the reader of the constraint from VL99, which for $\Omega_0 = 0.35$ gave $\sigma_8 = 0.92$ within [0.73, 1.12] at 95 per cent confidence. By contrast, in Seljak (2002) a value of $\sigma_8 = 0.70$ was obtained, based on the cluster mass to X-ray temperature relation derived in Finoguenov et al. (2001) from cluster data.

The calculation of σ_8 performed in this paper is substantially different from that carried out in VL99: the semi-analytical modelling featured a change in the normalization of the assumed cluster mass–temperature relation and in the shape of the assumed cluster mass function; a different observational data set was used; and the method of estimating σ_8 from Monte Carlo simulations differed from the previous likelihood-type calculation, where no dispersion in the cluster relations was considered. Although the most probable value for σ_8 is quite different in both cases, the 95 per cent confidence intervals happen to be very similar.

In order to find the most important factors behind the different results, we ran several Monte Carlo simulations. First, we found that the inclusion of dispersion in the mass–temperature relation at the level considered in this paper does not seem to make much difference. Secondly, and more surprisingly, we found that replacing the Evr02 mass function with the Press–Schechter or the Jen01 mass function also changes the most probable value for σ_8 by less than 2 per cent. This appears in contradiction with claims in the literature, including our own (Wu 2001; Pierpaoli et al. 2001; Viana, Nichol & Liddle 2002), that the choice of mass function can change σ_8 by 5–10 per cent. However, that statement is only true if we keep the mass–temperature relationship unchanged, but in fact these different mass functions refer to different masses; Evr02 gives the number density of haloes with mass M_{200}, Press–Schechter uses the virial mass which for the cosmology assumed here is about M_{108}, and the Jen01 mass function corresponds to M_{63} for the same cosmology. If we use the NFW cluster density profile to scale these mass functions to the same mass definition (e.g. the virial mass), most of the difference in σ_8 disappears. We note, however, that this similarity of results may be specific to the cosmology adopted here.

A change that does make a difference is that, compared to VL99, this paper uses a much lower normalization of the cluster mass to X-ray temperature relation. So that we could determine the influence of such normalization on our results, and be able to compare them more easily with others, we calculated the dependence of the most probable σ_8 on the value of the assumed present-day mass (M_{200}@5 keV) of a 5-keV cluster (approximately the median temperature of the HIFLUGCS subsample we work with). Taking the index of the cluster mass to X-ray temperature relation to be the standard 1.5, we found

$$\sigma_8 = 0.37 + 0.11 \times \left(\frac{M_{200}@5\,\mathrm{keV}}{10^{14}\,h^{-1}\,\mathrm{M}_\odot} \right)^{0.83} . \quad (9)$$

Note that in our main calculation we assumed M_{200}@5 keV $= 4.83 \times 10^{14}\,h^{-1}\,\mathrm{M}_\odot$, for an index of 1.54. Given that in VL99 it was assumed M_{200}@5keV $= 7.67 \times 10^{14}\,h^{-1}\,\mathrm{M}_\odot$, we obtain $\sigma_8 = 0.97$ as the value we would expect from VL99 if the only significant difference between the analyses was that change in the normalization. Compared with the VL99 value of $\sigma_8 = 0.92$, this seems to be correct, with the HIFLUGCS subsample we consider favouring just a slightly higher normalization than the Henry & Arnaud (1991) data set used in VL99. Although it is difficult to untangle all the competing effects, we suspect that together the new analysis method and the HIFLUGCS data set allow for a much better estimate of incompleteness which would help explain why they favour a higher normalization.

Turning to comparison with other work, the reason why Seljak (2002) obtained a significantly smaller value for σ_8 with relation to VL99 (to which it is more easily compared) is the assumption at fixed cluster temperature of a mass that is about 2.4 times lower than that assumed in VL99, although this effect is mitigated by Seljak's assumed local cluster abundance at about 6 keV (from Pierpaoli et al. 2001), which was higher than that of VL99. In this paper we too have a cluster mass at 6 keV which is much smaller than VL99, but the reduction is by a smaller factor of 1.6.

As we were completing this work, a paper by Pierpaoli et al. (2003) appeared in which a similar analysis to ours and that in Ikebe et al. (2002) was carried out. The observed cluster sample is also derived from HIFLUGCS, but otherwise they use a different approach to obtain constraints on σ_8. While both here and in Ikebe et al. (2002) an attempt is made to constrain σ_8 simultaneously with the relation of X-ray temperature to luminosity, in Pierpaoli et al. (2003) such a relation is assumed a priori (to be that given by expression 3 in Ikebe et al. 2002). We have attempted to reproduce the constraint obtained for σ_8 by Pierpaoli et al. (2003) when they derive the observed cluster sample just from HIFLUGCS. Such a constraint can be read from the full line in figs 4 and 5 of Pierpaoli et al. (2003). Concentrating on the case of $\Omega_0 = 0.35$, and performing an analysis equivalent to that in Pierpaoli et al. (2003), taking care to make the same assumptions and apply the selection criteria in the same manner, but using the 2D KS method instead, we found a most probable value for σ_8 and the 90 per cent confidence interval very similar to theirs (a slight overestimation by 0.02). On the other hand, if we just change in our own analysis the relation of cluster mass to X-ray temperature so that M_{200}@5 keV $= 3.82 \times 10^{14}\,h^{-1}\,\mathrm{M}_\odot$ at present and its index to 1.5, as in Pierpaoli et al. (2003), the result for σ_8 is again very similar (about 0.71) to that obtained in Pierpaoli et al. (2003). Clearly, the most significant factor leading to the different HIFLUGCS based result obtained here and in Pierpaoli et al. (2003) regarding σ_8 is the difference in the normalization of the relation of cluster mass to X-ray temperature.

Our results do not indicate a dramatic reduction in σ_8 derived from the abundance of X-ray clusters. Several other recent analyses have favoured low σ_8, for instance from 2dF and cosmic microwave background (CMB) data (Efstathiou et al. 2002; Lahav et al. 2002), from using weak lensing to estimate cluster masses (Viana et al. 2002), and from the local X-ray cluster luminosity function (Allen et al. 2002), but those are at least marginally compatible with our present result given the uncertainties. Indeed, results from *WMAP* have forced a modest increase in estimates of σ_8 via CMB data

(Spergel et al. 2003). Our estimated value for σ_8 is compatible with all published weak lensing measurements (e.g. Bacon et al. 2002; Hökstra, Yee & Gladders 2002; Refregier, Rhodes & Groth 2002; Van Waerbeke et al. 2002), although only marginally with the very low results of Brown et al. (2003), Hamana et al. (2003) and Jarvis et al. (2003), as well as at the other extreme with that of Maoli et al. (2001).

In the near future, a decrease in the uncertainty in the estimation of σ_8 from X-ray clusters could come from essentially two sources. On the theoretical side, it would be important to reliably estimate the X-ray luminosity of clusters using hydrodynamical N-body simulations. This would enable us to bypass the X-ray temperature as the cluster mass estimator. Although temperature is more reliable, it ends up not being as useful as it could be due to the fact that all cluster catalogues are flux-limited instead of temperature selected, so an estimation of the cluster X-ray flux always needs to be made. On the observational side, both an improvement in the temperature determination and an increase in the range of redshift probed (i.e. a decrease in the X-ray flux detection limit) would help bring down the uncertainty in the estimation of σ_8. Hopefully, both can be achieved with the X-ray satellites *Chandra* and *XMM–Newton*. In particular, it is expected that the serendipitous cluster survey *XCS* (Romer et al. 2001), to be assembled with *XMM–Newton* data, will help greatly in both issues.

ACKNOWLEDGMENTS

The simulations used in this paper were carried out on the Cray-T3E at the Edinburgh Parallel Computing Centre (EPCC) as part of the Virgo Consortium programme of investigations into the formation of structure in the Universe. STK is supported by the Particle Physics and Astronomy Research Council (PPARC) and ARL in part by the Leverhulme Trust. During the initial preparation of this paper, OM was supported by a Development and Promotion for Science and Technology (DPST) scholarship from the Thai government and PAT was a PPARC Lecturer Fellow. PTPV acknowledges the financial support of FCT through project POCTI/FNU/43753/2001 (partially funded through FEDER). We thank Elena Pierpaoli for useful discussions.

REFERENCES

Allen S. W., Schmidt R. S., Fabian A. C., 2001, MNRAS, 328, L37
Allen S. W., Schmidt R. S., Fabian A. C., Ebeling H., 2002, MNRAS, 342, 287
Bacon D., Massey R., Refregier A., Ellis R., 2003, MNRAS, 344, 673
Bennett C. L. et al., 2003, ApJS, 148, 1
Blanchard A., Sadat R., Bartlett J. G., le Dour M., 2000, A&A, 362, 809
Brown M. L., Taylor A. N., Bacon D. J., Gray M. E., Dye S., Meisenheimer K., Wolf C., 2003, MNRAS, 341, 100
Bryan G. L., Norman M. L., 1998, ApJ, 495, 80 (BN98)
Couchman H. M. P., Thomas P. A., Pearce F. R., 1995, MNRAS, 452, 797
Davis M., Efstathiou G., Frenk C. S., White S. D. M., 1985, ApJ, 292, 371
Diego J. M., Martinez-Gonzales E., Sanz J. L., Cayon L., Silk J., 2001, MNRAS, 325, 1533
Dodelson S. et al. (the SDSS collaboration), 2002, ApJ, 572, 140
Efstathiou G. et al. (the 2dF collaboration), 2002, MNRAS, 330, L29
Eke V. R., Cole S., Frenk C. S., 1996, MNRAS, 282, 263
Evrard A. E., 1989, ApJ, 341, L71
Evrard A. E., Metzler C. A., Navarro J. F., 1996, ApJ, 469, 494 (EMN96)
Evrard A. E. et al., 2002, ApJ, 573, 7 (Evr02)
Fasano G., Franceschini A., 1987, MNRAS, 225, 155
Finoguenov A., Reiprich T. H., Böhringer H., 2001, A&A, 368, 749
Hamana T. et al., 2003, ApJ, in press (astro-ph/0210450)
Henry J. P., 1997, ApJ, 489, L1
Henry J. P., 2000, ApJ, 534, 565
Henry J. P., Arnaud K. A., 1991, ApJ, 372, 410
Hökstra H., Yee H. K. C., Gladders M. D., 2002, ApJ, 577, 595
Holder G., Haiman Z., Mohr J., 2001, ApJ, 560, L111
Ikebe Y., Reiprich T. H., Böhringer H., Tanaka Y., Kitayama T., 2002, A&A, 383, 773
Jarvis M., Bernstein G., Jain B., Fischer P., Smith D., Tyson J. A., Wittman D., 2003, AJ, 125, 1014
Jenkins A. R., Frenk C. S., White S. D. M., Colberg J. M., Cole S., Evrard A. E., Couchman H. M. P., Yoshida N., 2001, MNRAS, 321, 372 (Jen01)
Lacey C., Cole S., 1994, MNRAS, 271, 676
Lahav O. et al. (the 2dF team), 2002, MNRAS, 333, 961
Maoli R., Van Waerbeke L., Mellier Y., Schneider P., Jain B., Bernardeau F., Erben T., Fort B., 2001, A&A, 368, 766
Marshall H. L., Avni Y., Tananbaum H., Zamorani G., 1983, ApJ, 269, 35
Mathiesen B. F., Evrard A. E., 2001, ApJ, 546, 100 (ME01)
Muanwong O., Thomas P. A., Kay S. T., Pearce F. R., 2002, MNRAS, 336, 527 (MTKP02)
Navarro J. F., Frenk C. S., White S. D. M., 1995, MNRAS, 275, 720
Navarro J. F., Frenk C. S., White S. D. M., 1996, ApJ, 462, 563
Navarro J. F., Frenk C. S., White S. D. M., 1997, ApJ, 490, 493
Oukbir J., Blanchard A., 1992, A&A, 262, L21
Peacock J. A., 1983, MNRAS, 202, 615
Pearce F. R., Couchman H. M. P., 1997, New Astron., 2, 411
Peebles P. J. E., 1993, Principles of Physical Cosmology. Princeton University Press, Princeton
Percival W. J. et al. (the 2dF collaboration), 2001, MNRAS, 327, 1297
Pierpaoli E., Scott D., White M., 2001, MNRAS, 325, 77
Pierpaoli E., Borgani S., Scott D., White M., 2003, MNRAS, 342, 163
Press W. H., Schechter P., 1974, ApJ, 187, 425
Press W. H., Teukolsky S. A., Vetterling W. T., Flannery B. P., 1992, Numerical Recipes. Cambridge University Press, Cambridge
Refregier A., Rhodes J., Groth E. J., 2002, ApJ, 572, L131
Reiprich T. H., Böhringer H., 2002, ApJ, 567, 716
Romer A. K., Viana P. T. P., Liddle A. R., Mann R. G., 2001, ApJ, 547, 594
Seljak U., 2002, MNRAS, 337, 769
Sheth R. K., Mo H. J., Tormen G., 2001, MNRAS, 323, 1
Spergel D. N. et al., 2003, ApJS, 148, 175
Sutherland R. S., Dopita M. A., 1993, ApJS, 88, 253
Szalay A. S. et al. (the SDSS collaboration), 2003, ApJ, 591, 1
Thomas P. A., Muanwong O., Pearce F. R., Couchman H. M. P., Edge A. C., Jenkins A., Onuora L., 2001, MNRAS, 324, 450 (T01)
Thomas P. A., Muanwong O., Kay S. T., Liddle A. R., 2002, MNRAS, 330, L48
Van Waerbeke L., Mellier Y., Pello R., Pen U.-L., McCracken H. J., Jain B., 2002, A&A, 393, 369
Viana P. T. P., Liddle A. R., 1996, MNRAS, 281, 323
Viana P. T. P., Liddle A. R., 1999, MNRAS, 303, 535 (VL99)
Viana P. T. P., Nichol R. C., Liddle A. R., 2002, ApJ, 569, L75
White S. D. M., Efstathiou G., Frenk C. S., 1993a, MNRAS, 262, 1023
White S. D. M., Navarro J. F., Efstathiou G., Frenk C. S., 1993b, Nat, 366, 429
Wu J.-H. P., 2001, MNRAS, 327, 629

This paper has been typeset from a TEX/LATEX file prepared by the author.